Fire Dynamics for Mass Timber Compartments

Carmen Gorska[a*], Juan P. Hidalgo[b], Jose L. Torero[b]

[a]The University of Queensland, Building 49, Staff House Rd, St Lucia QLD 4072, Australia, c.gorskaputynska@uq.edu.au

[b]The University of Queensland, Building 49, Staff House Rd, St Lucia QLD 4072, Australia, j.hidalgo@uq.edu.au

[c]University College London, Chadwick building, 104 Gower street, London WC1E 6DE, UK, j.torero@ucl.ac.uk

*Corresponding author

Highlights:

- Gas-phase temperatures in timber compartments
- Flow velocities induced by timber surfaces in compartment fires
- Burning rate of timber in a compartment fire environment
- Compartment fire regime change due to the introduction of timber lining

Abstract:

Since Engineered Wood Products (EWPs) have entered the building industry as structural elements, several fire safety concerns have arisen, especially for high-rise structures.

The combustible nature of timber suggests that the current knowledge on compartment fire dynamics might not apply to compartments with timber boundaries, due to the increased fuel load and its redistribution across the compartment.

In order to fill this knowledge gap, 24 medium-scale timber compartments have been executed to characterise the fire dynamics when timber members are present.

This experimental campaign provides data about the gas-phase temperatures, the flow fields at the opening, the burning behaviour of timber and its contribution to the total heat release rate. This data is then compared to current tools that predict the fire development in conventional compartments.

This comparison dismantles the limitations of the current framework, and the subsequent analysis proposes several changes to include the effect of burning timber elements. It is concluded that gas flow velocities increase with the amount of more timber present in the compartment. Therefore the fire transitions to a new regime where the gases do not have enough time to mix and react inside the compartment, the temperatures decrease and the horizontal velocities at the opening increase.

Keywords: Compartment Fires; Heat Release Rate; Timber Buildings

1 Introduction

The modern building industry is continuously seeking for materials more sustainable than steel and concrete, aesthetically appealing and economical. As a response to these incentives, Engineered Wood Products (EWP) [1, 2] have entered the construction market with their use delivering a new typology generally referred to as mass timber construction. This new manufacturing technology has enabled the use of timber in high-rise building construction due to its enhanced properties and constructability. For high-rise structures, the fire safety strategy relies on compartmentation, which allows containing the fire within the compartment of fire origin using physical barriers. Successful compartmentation prevents the fire from spreading horizontally and vertically, minimises the number of structural elements exposed to heating and ensures that the staircase is free from smoke and heat for a safe evacuation [3]. Mass timber construction introduces unique fire hazards that need to be considered explicitly in building design. These hazards correspond to increased fuel load, the potential for fire spread through the building, and the structural collapse due to the combustible nature of timber structures.

The presence of a compartment results in a distinctive fire development, known as compartment fire dynamics. Comprehensive reviews of this phenomenon can be found in [4-8]. The classical evolution of a compartment fire has three characteristic stages: fire growth, fully-developed fire and decay phase. The fully-developed fire is the stage that can potentially compromise compartmentation and structural integrity since it presents the highest temperatures. A review of the current framework to characterise this stage is presented below.

1.1 Compartment gas-phase temperatures

Thomas *et al.* [9] conducted a detailed study of fully-developed fire compartments with different geometries. They developed a correlation to predict the maximum gas-phase temperature inside the compartment as a function of the opening factor (O_F), with the intent of determining the thermal load on the structure and compartment boundaries.

$$O_F = \frac{A_T}{A_w H^{1/2}} \tag{1}$$

Where A_T is the area of the compartment boundaries excluding the floor, and A_w and H are the area and height of the opening, respectively. This correlation is presented in Fig. 1.

This definition of the opening factor represents the energy balance inside the controlled volume of the compartment: heat losses through the compartment walls (A_T) vs the heat generation represented by the air inflow accommodated by the opening ($A_w H^{1/2}$). This ratio determines the energy stored by the gases inside the compartment which is a function of their temperature.

The compartment fire framework was developed for non-combustible materials [9]; thus the extension of this methodology to mass timber structures needs to be fully justified.When EWP are used to construct walls, floors, columns and beams they will participate in the fire influencing its behaviour beyond the impact of the fuel associated with combustible furnishings. Despite the very dramatic effects of timber on the compartment fire behaviour, these effects have not been systematically studied. This research focuses on predicting the fully-developed stage to adequately define the thermal boundary conditions for the structural and compartmentation design in timber buildings.

1.2 Compartment fire regimes

The opening factor separates compartments fires behaviour into two different regimes.

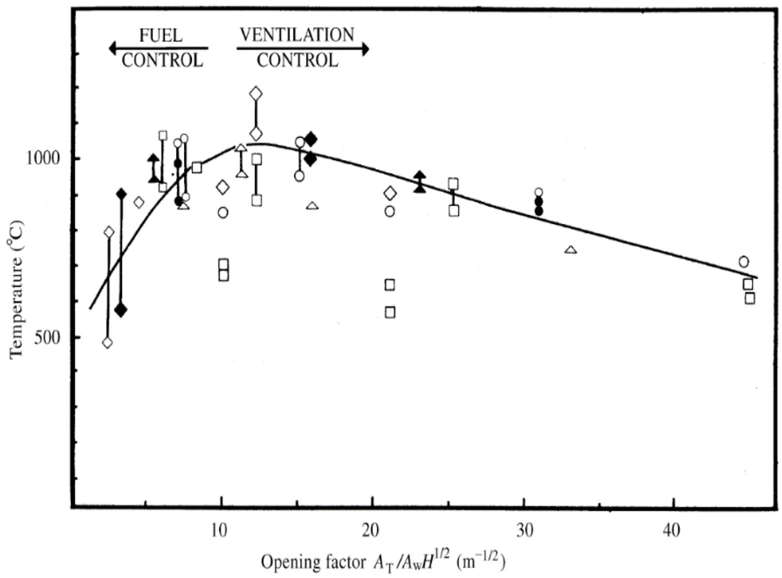

Fig. 1. Temperatures registered inside the compartment vs the opening factor. Extracted from [8]

Regime I, is controlled by the area of the opening. In this regime, the vents are small, the combustion is fuel-rich, and a significant portion of heat is released outside in the form of external flaming. For geometries that satisfy Regime I, it is assumed uniform temperatures inside the compartment, negligible momentum and a static pressure differential across the opening, which controls the gas flow in and out of the compartment [5, 10, 11]. Consequently, the internal temperatures decrease with a smaller opening, since less air (i.e. oxygen) can flow inside to feed the combustion.

Conversely, Regime II, has large openings so that the smoke can evacuate easily. The flow induced by the fire pushes the hot gasses out and consequently draws air in the compartment. Therefore, the pressure difference caused by the fire is more significant than the static pressure difference across the opening. This regime is considered momentum-driven and a comprehensive set of transport equations needs to be solved to establish the temperature distribution within the compartment [10].

As a result of different forces driving each regime, the assumptions for Regime I are not valid for Regime II, and therefore, each regime should be solved independently. To adequately predict the fire development in timber structures, it is necessary to know if compartments with EWP will behave according to the regime defined by their opening factor and if not, characterise the effect of the timber members.

1.3 Assumptions of the compartment fire framework

Two assumptions have been identified that could be inadequate for compartments constructed with EWP:

1. The methodology to predict the maximum temperatures presented in section 1.2 assumes that heat is lost through all the boundaries of the compartment except the opening and the floor covered in burning fuel. However, this might not be the case for timber surfaces, since the timber is very likely to ignite and provide additional heat to the compartment instead of acting as a heat-sink.
2. The change from Regime I to Regime II and the subsequent increase in the velocity field is only related to the geometrical dimensions of the compartment. Nevertheless, a burning timber wall inside the compartment can strengthen or suppress the buoyant flows affecting the resulting velocities. For an opening factor in Regime I, this effect could break the assumption of negligible velocities inside the compartment and a flow exchange driven by a static pressure difference at the opening.

This paper presents an experimental series to analyse the fire dynamics in compartments with exposed timber walls and ceiling. The validity of the compartment framework assumptions is assessed by studying the heat release rate contributions from the timber, temperatures in the gas-phase, and velocity fields at the opening.

2 Methodology

2.1 Compartment configuration

To investigate the effect of exposed timber walls on the compartment fire dynamics, 24 medium-scale compartments experiments were conducted. The compartments were constructed with Radiata Pine Cross-Laminated Timber (CLT) sourced from XLam and with a density of 0.425 g/mm^3 where CLT is a type of EWP. For this experimental campaign, the CLT lamellas had a thickness sequence of 45-20-20-20-45 mm. Fig. 2 shows schematics of the cuboid compartment which had internal dimensions of 50 x 50 x 37 cm and a single opening of 30 x 28 cm.

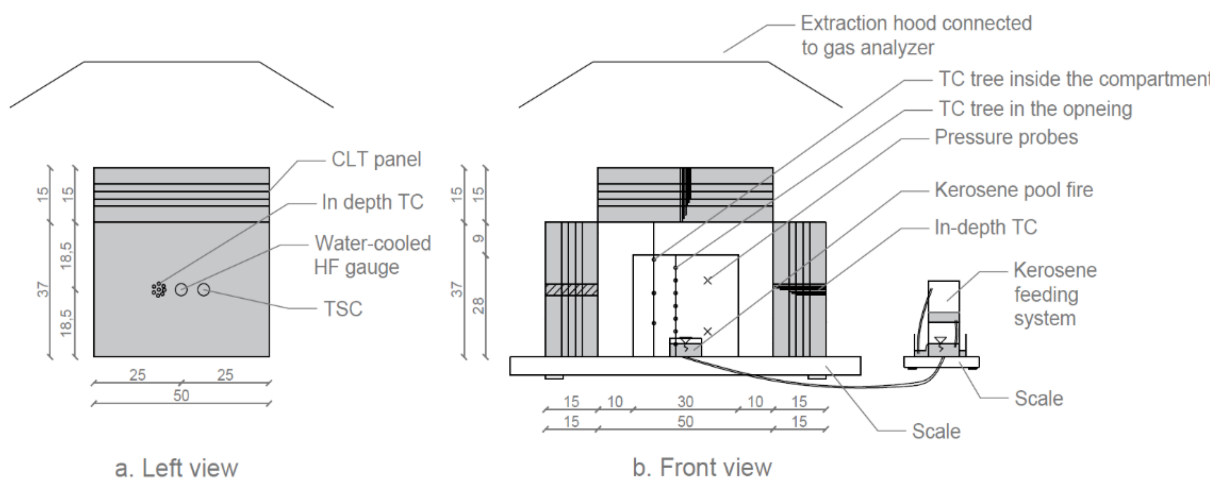

Fig. 2. Experimental setup. TC: Thermocouple, HF gauge: Heat Flux gauge and TSC: ThinSkin Calorimeters.

The opening factor was 18.43 $m^{-1/2}$ calculated as per Eq. 1. According to [4, 9, 10] this geometry and used materials guarantee flashover while achieving almost the highest gas-phase temperatures inside the compartment.

Eight different configurations of exposed timber surfaces were tested. The walls that were not meant to participate in the fire were protected with two layers of 12 mm Knauf FireShield plasterboard. Each configuration was repeated three times and the designs were as listed below:

Configuration	Exposed CLT Area [-]
1. Baseline	0
2. Exposed C	0.21
3. Exposed LW	0.16
4. Exposed LW, C	0.38
5. Exposed LW, BW	0.33
6. Exposed LW, BW, C	0.54
7. Exposed LW, BW, LW2	0.49
8. Exposed ALL	0.7

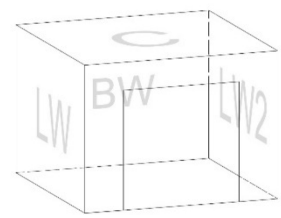

Fig. 3. Compartment walls legend
LW: Lateral Wall, BW: Back Wall
C: Ceiling

For normalising purposes, the exposed CLT area is expressed as a fraction of the total area of the compartment boundaries, excluding the area of the opening.

$$Normalised\ CLT\ Area = \frac{\sum A_{CLT,exposed}}{A_{TOTAL}} \quad (2)$$

2.2 Fire scenario

Preliminary experiments [12, 13] demonstrated that 10 min after flashover the compartment reached steady-state, which was defined with the total heat release rate (HRR), the gas-phase temperature and the charring rate of the CLT panels. The first timber-lamella fall off (delamination) occurred after approximately 30min. Therefore, the duration of the fully-developed fire was set to 20 min. To guarantee steady-state readings for all the configurations only the last 5 min of the fully-developed fire was considered for the analysis.

The fuel consisted of a 9 cm diameter kerosene pan, which has a similar soot production to plastic and cellulosic fires and represents a fuel load comparable to an office building.

A kerosene feeding system was designed to continually feed the kerosene pool fire inside the compartment (Fig. 2). This feeding system allowed to keep a constant liquid-level, and to terminate the test at the desired time. Most importantly, the scale under the system provided the mass loss rate of the kerosene pool fire, ($MLR_{kerosene}$). Consequently, this system permitted to calculate the HRR from the CLT panels (HRR_{CLT}) by decoupling the $HRR_{Kerosene}$ from the HRR_{TOTAL} which was measured with a calorimeter above the experimental setup.

$$HRR_{Kerosene} = MLR_{kerosene} \cdot \Delta H_{c,kerosene} \quad (3)$$

$$HRR_{CLT} = HRR_{TOTAL} - HRR_{Kerosene} \quad (4)$$

where $MLR_{kerosene}$ is the mass loss rate of the kerosene pool fire in [g/s], and $\Delta H_{c,kerosene}$ is the heat of combustion of kerosene in [kJ/g].

2.3 Instrumentation

The following instrumentation was used to characterise the compartment fire dynamics (Fig. 2):

- A K-type thermocouple (TC) tree was placed at the back of the compartment, with three TCs uniformly distributed along the compartment's height: 9.25, 18.5 and 27.75 cm from the floor.
- A TC tree was installed at the opening, with seven TCs uniformly distributed along the opening's height: 3.5, 7, 10.5, 14, 17.5, 21 and 24.5 cm from the floor.
- TCs were embedded in each CLT panel to measure the temperature profile evolution. The depths of the TCs in respect of the external surface were: 0, 85, 95, 105, 130, 140, 145 and 147 mm.
- Two pressure probes were placed at the opening plane to capture the inflow and outflow gas velocities. The probes were placed at ¼ and ¾ of the opening's height.
- A calorimeter above the whole experimental setup extracted all the combustion products. The calorimeter measured the concentration of O_2, CO and CO_2. The Total Heat Release Rate, HRR_{TOTAL} was calculated using the oxygen consumption method [14].

2.4 Analysis methods to evaluate the CLT pyrolysis rate

In steady-state conditions, the pyrolysis rate can be defined as the velocity of the pyrolysis front progressing through the timber. This velocity can be calculated with the position of the pyrolysis isotherm at two different times, and by dividing the distance between both positions by the time delay, Equation 5:

$$\dot{p} = \frac{d_{i+\Delta t} - d_i}{\Delta t} \tag{5}$$

where $\dot{p}$ [mm/min] is the pyrolysis rate, d_i [mm] is the position of the pyrolysis isotherm at time i, and Δt [min] is the time interval.

The intersection point of the pyrolysis isotherm with the temperature profile determines the position of the pyrolysis front at a given time. Therefore it is required to interpolate the temperatures between the in-depth thermocouple readings to estimate a continuous temperature profile in the timber. However, there are several methods to perform the interpolation between points and each method represents a different heat transfer condition.

Three methods have been evaluated to fit a temperature profile curve into the data points.

1. Linear interpolation: It is the solution for steady-state conduction, where the characteristic charring time (τ_{CH}) is considerably smaller than the characteristic time for steady-state (τ_{SS}) : $\tau_{CH} \ll \tau_{SS}$
2. Polynomial interpolation: It represents transient conduction using the t^2- Approximation. It is used for the condition where $\tau_{CH} \approx \tau_{SS}$.
3. Error function solution: It is the solution to the generic heat diffusion equation:

$$\frac{\partial^2 T}{\partial x^2} = \frac{1}{\alpha}\frac{\partial T}{\partial t} \tag{6}$$

It represents an ablation front where the heat of pyrolysis (ΔH_{pyr}), and heat of water vaporisation (ΔH_{vapor}) are considerably smaller than the external heat flux ($\dot{q}''_{ext}$):

$$\Delta H_{pyr} \;\&\; \Delta H_{vapor} \ll \dot{q}''_{ext} \tag{7}$$

The pyrolysis and water vaporization fronts are very close to each other and can be considered as one front. This allows assuming that the material behind this front is virgin timber. Therefore, one curve can be fitted to describe the whole profile instead of several curves going from point to point as in method 1 and 2.

To solve Eq. 6 the following assumptions were set: (1) Transient conduction problem, (2) semi-infinite solid and (3) constant surface condition: $T(0,t) = T_s$.

Thus, the solution to determine the temperature profile is as follows:

$$T(x) = \operatorname{erf}\left(\frac{x}{L_c}\right)(T_i - T_s) + T_s \tag{8}$$

Where L_c is the characteristic length and the computed variable to fit the temperature profile into each set of temperature points, (x = thermocouple depth vs T_s= temperature).

Fig. 4. presents the temperature profiles for an exemplary test which were calculated using the three different methods. The profiles are measured with a 5 minutes time delay. The figure illustrates the intersection method of the pyrolysis isotherm with the temperature profiles.

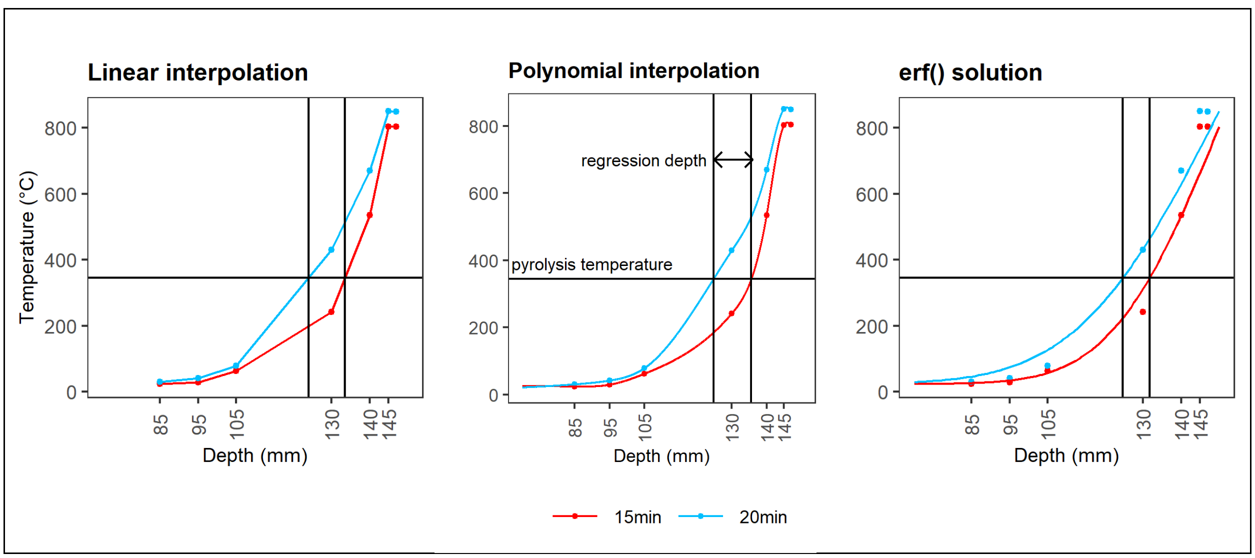

Fig. 4. Temperature profiles in the CLT panels at two different time of the fully-developed fire. Three different methods to calculate the profiles representing three different burning scenarios.

To validate the accuracy of each method, the total pyrolysis regression was compared with the HRR_{CLT}, since the following proportionality should be met: $\dot{m}_{pyrolysis} \propto HRR_{CLT}$ HRR_{CLT} was decoupled thanks to the kerosene feeding system as presented in section 2.2. Each timber surface was assumed to have a uniform regression rate across its area. Thus, the total pyrolyzing volumetric rate of each configuration can be calculated as per Eq. 9:

$$\dot{p}''' = \sum_{i=1}^{n} A_{CLT,i} \cdot \dot{p}_i \tag{9}$$

where $\dot{p}'''$ [mm^3/min] is the total pyrolyzing volumetric rate, $A_{CLT,i}$ [mm^2] is the exposed timber area of surface i, and $\dot{p}_i$ [mm/min] is the pyrolysis rate of surface i.

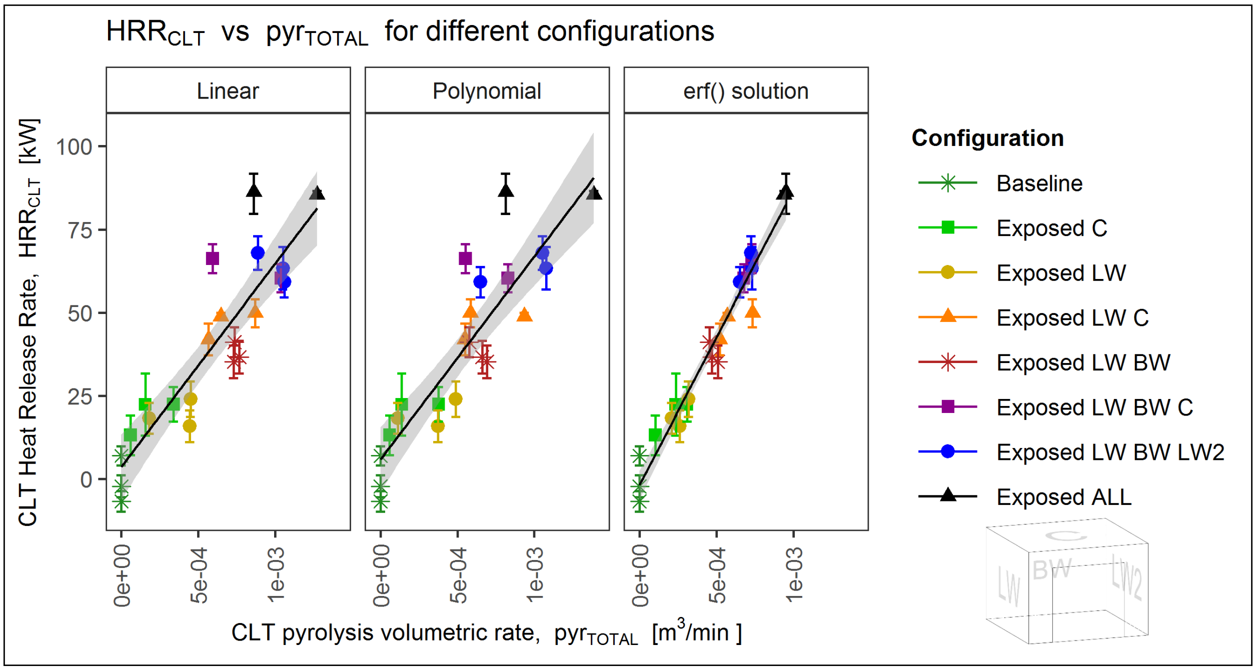

Fig. 5. Linear model represting the relationship between the volumetric pyrolysis rate and the HRR from the CLT.

Fig. 5 indicates that the relation of the volumetric pyrolysis rate to HRR_{CLT} is best represented by the error function method, as it presents the smallest 95% confidence interval. Therefore, this method is adopted for the subsequent analysis.

3 Results

3.1 Gas-phase temperature profiles

Fig. 6 illustrates the evolution of the temperature profiles as more CLT is being exposed. The figure indicates that the smoke layer height descends as more CLT contributes to the fire since lower heights have higher temperatures. Additionally, an interesting phenomenon is observed in the profiles' shape. As more timber is being exposed, the upper thermocouples start to get colder than the middle ones. This phenomenon is firstly observable in the thermocouple tree placed at the opening, but eventually, the internal thermocouples present the same behaviour. This observation indicates that the height of the hottest layer is not below the ceiling, but closer to the neutral plane height which descends as more timber is being exposed.

As a result of these observations, Fig. 6 is the first indicator of a change in the fire regime induced by timber lining. The results demonstrate that the smoke layer height descends despite the compartments having the same dimensions and that the gases do not stratify from hottest to coolest. The latter observation suggests the presence of a new mechanism that induces flows and affects the temperature profiles, preventing them from adopting the conventional shape,

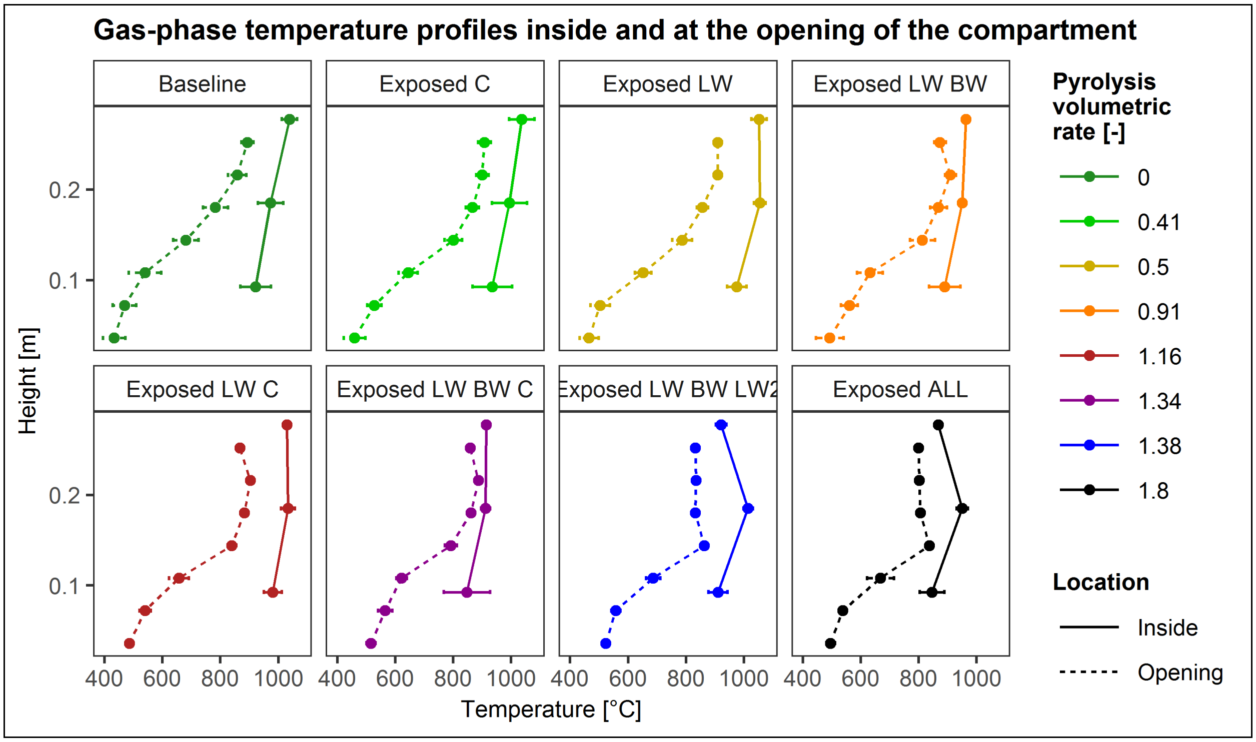

Fig. 6. Temperature profiles inside the compartment and at the opening for different CLT configurations

3.2 Mean gas-phase temperatures

This section presents how the internal mean temperatures and opening factor relate to the fitted curve proposed by Thomas *et al.* plotted in Fig. 1.

Firstly, using the correlation from Fig. 1, a theoretical temperature was defined based on the opening factor from the compartment ($O_{F,ref}$). These reference values were used to normalize the experimental results:

$$O_{F,ref} = 18.43\ m^{1/2} \quad \rightarrow \quad T_{ref} = 990\ ℃$$

Fig. 7 presents the mean gas-phase temperatures during steady-state for all the tested configurations. The data deviate considerably from the theoretical temperature proposed by Thomas *et al.*

The Baseline case falls pretty close to the theoretical temperature, T_{ref}, meaning that the Thomas *et al.* methodology predicts satisfactorily the temperatures for the type of compartment for which it was designed: a compartment with non-combustible boundaries. The following two configurations, Exposed C and Exposed LW, have considerably higher temperatures than T_{ref}, and all the subsequent configurations, with more and more exposed timber, fall bellow the theoretical value.

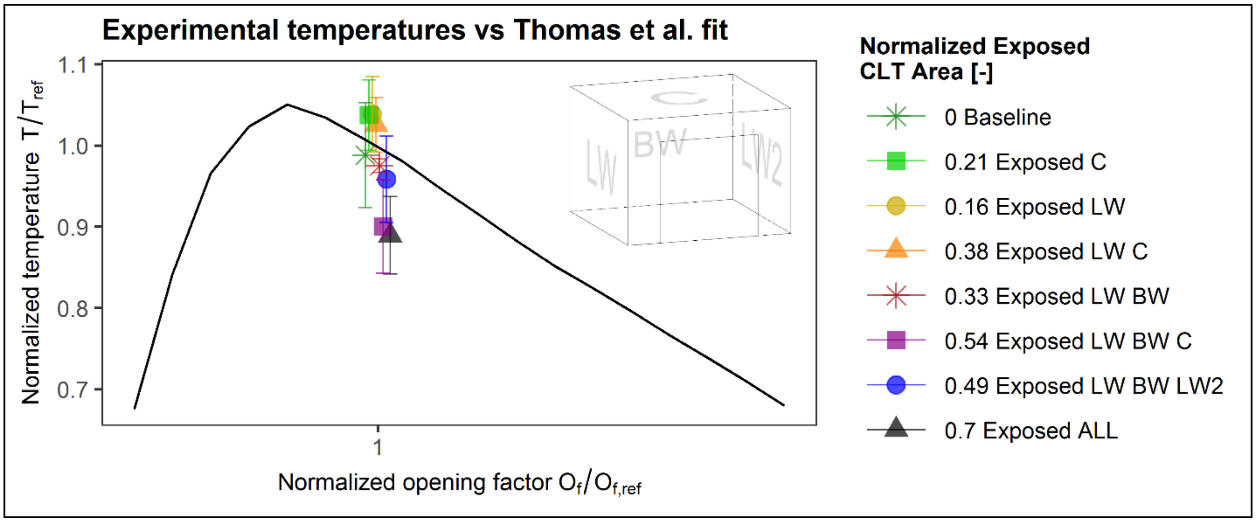

Fig. 7. Normalized mean gas-phase temperarues inside the compartment achieved in the different CLT configurations, compared to the fitted curve proposed by Thomas *et al.*

It is surprising to observe that increasing the exposed timber area results in an increase in temperatures only until a certain point, after which the temperatures start to decay.

Fig. 7 confirms that compartments with timber lining do not meet the first assumption of Thomas *et al.* framework presented in section 1.3, since the gas-phase temperatures are not predicted accurately, except for the Baseline case. Thus, the results suggest again a regime change. Eq. 1 should be modified to include the effect of timber walls in the calculation of the opening factor, so it represents accurately the energy balance and temperatures developed inside the fully-developed compartment fire.

3.3 Flow velocities at the opening

The readings of the pressure probes that were placed at the opening are presented in **Error! Reference source not found.**. This experimental campaign developed a significant increase in velocities as more CLT panels were left exposed. This increase in velocities breaks the second assumption of Thomas *et al.* framework presented in section 1.3 regarding a mass flow exchange at the opening driven by a static pressure difference and a negligible momentum inside the compartment. For example, in Fig. 7, the Exposed ALL configuration presented the lowest mean temperature inside the compartment, for a problem driven by a static pressure difference, that should implicate the development of the lowest velocities as well. However, in **Error! Reference source not found.**, the same configuration presents the highest velocities at the opening when compared to the other scenarios. This behaviour is the evidence of the fact the burning CLT panels strengthen the buoyant flow inside the compartment, which accumulates under the ceiling and then is redirected towards the opening with increased velocity.

Therefore, **Error! Reference source not found.** shows another set of data that suggesting a shift of the fire dynamics towards a new regime with much larger velocities than the ones developed by a static pressure difference and the limited applicability of the framework to CLT compartments.

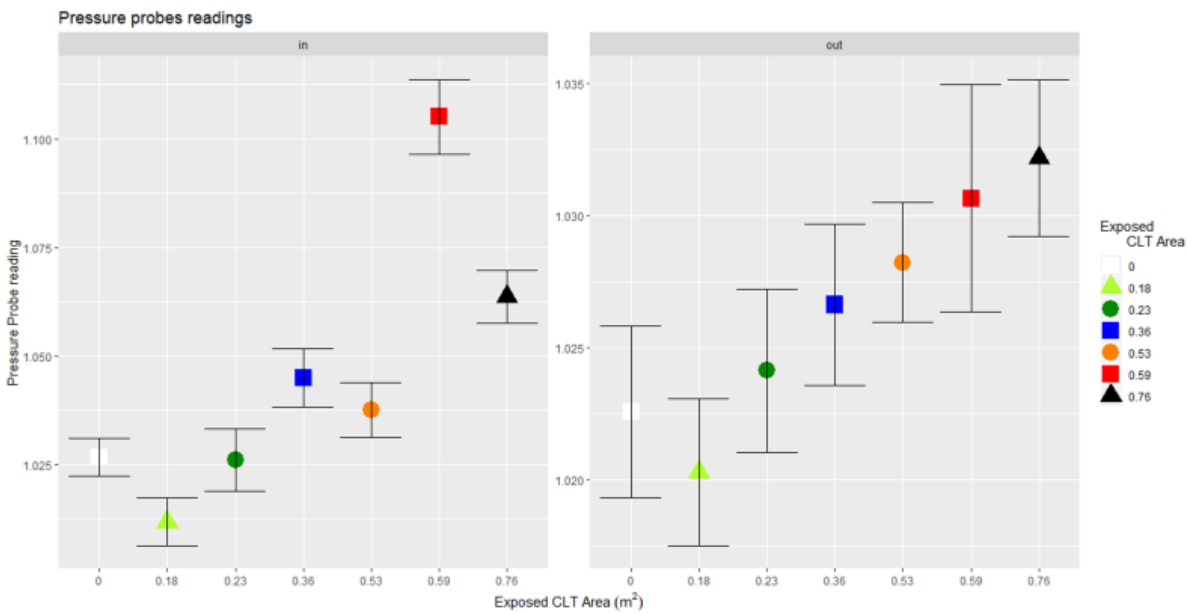

Fig. 8

4 Discussion

The experimental results reveal a regime change induced by burning CLT surfaces, and this change is not captured by the current framework. The prevailing limitations of the framework are associated to the definition of the area of heat losses for the opening factor and to the fire regime change, and all its implications, being related to the opening factor only.

Eq. 10 is a modification of Eq. 1, where the opening factor is modified to reduce A_T by the exposed CLT area (A_{CLT}). This way the heat losses term is corrected and it does not consider the CLT surfaces to behave as a heat-sinks.

$$O_{F,modified} = \frac{A_T - A_{CLT}}{A_W H^{1/2}} \qquad (10)$$

Fig. 9 presents the same data points as in Fig. 7 but using the modified opening factor. The figure shows a redistribution of the temperatures with good agreement to the initially fitted curve proposed by Thomas *et al.* [9]

The subtraction of the CLT area in Eq. 10 means that the increase of CLT area decreases the heat losses from the compartment. Smaller heat losses should imply an increase in temperatures. Therefore, the exposure of new CLT surfaces should result in a temperature increase, until the point where the adiabatic flame temperature is reached, beyond which the temperatures should plateau.

By contrast, these experiments indicate that the temperatures progressively start to decay and move towards Regime II. This transition is also confirmed with the increased velocities presented in **Error! Reference source not found.**, which are characteristic of this regime.

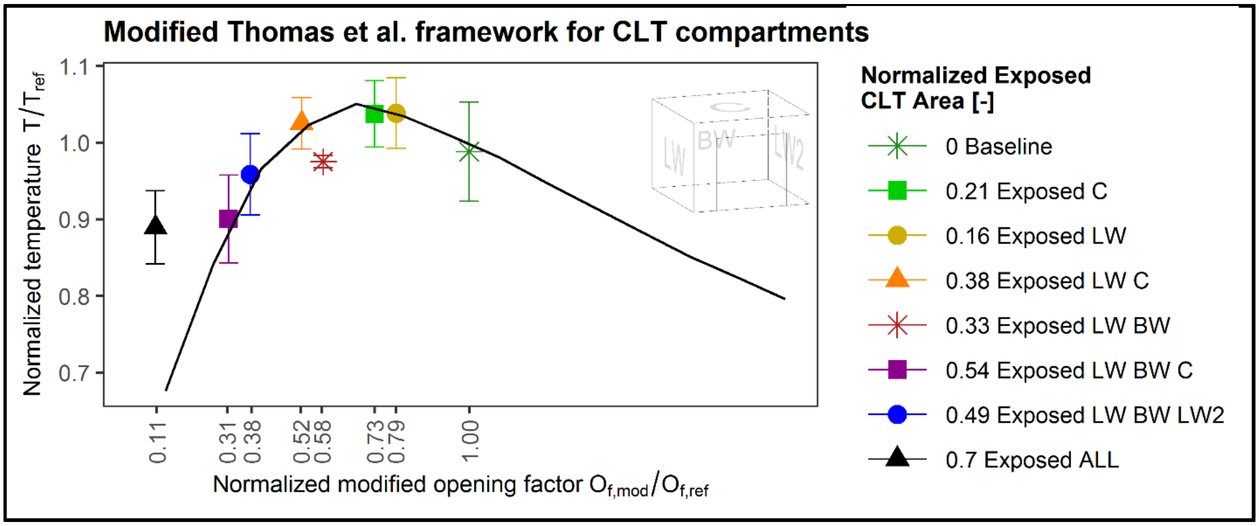

Fig. 9. Normalized mean gas-phase temperarues inside the compartment achieved in the different CLT configurations vs the modified O_F , compared to the fitted curve proposed by Thomas *et al.*

Therefore, all the results indicate that adding exposed timber surfaces shifts the fire dynamics towards a Regime II behaviour. It is important to note that for CLT compartments it is not the size of big openings and "excess" of oxygen that results in a Regime II fire, but the excess of pyrolysing gases from the CLT panels. Due to this difference, a Regime II fire induced by exposed CLT might be different from the conventional Regime II fire behaviour. Therefore, this research calls the later Regime-II-CLT.

The analysis of the velocity data together with the gas-phase temperature information allow describing the new Regime-II-CLT, where the induced momentum inside the compartment minimizes the time for the gases to flow outside, to the point where the gases are not able to efficiently mix inside. The consequence of inefficient mixing is demonstrated in the temperature profiles (Fig. 6), where the temperatures under the ceiling are lower for configurations with a large amount of exposed timber, suggesting that the combustion was not as efficient due to a lack of oxygen, and resulting in cooler mean temperatures as per Fig. 9.

This phenomenon is also observable in the pyrolysis rates of the different exposed timber walls presented in Fig. 10. It is noted that the ceiling has always a lower regression rate than the vertical walls, reflecting that it is the surface receiving less heat and oxygen. Consequently, it is not accurate to normalise the configurations as a function of exposed area, Eq. 2, as it does not consider the variation of pyrolysis rate for different surfaces. Therefore, it is proposed to use the total volumetric pyrolysis rate Eq. 11, as a variable to normalise the different configurations:

$$\bar{p} = \dot{p}'''/\widehat{\dot{p}'''} \quad (11)$$

Where $\bar{p}$ [-] is the normalised volumetric pyrolysis rate, and $\widehat{\dot{p}'''}$ [mm^3/min] is the average pyrolysis volumetric rate.

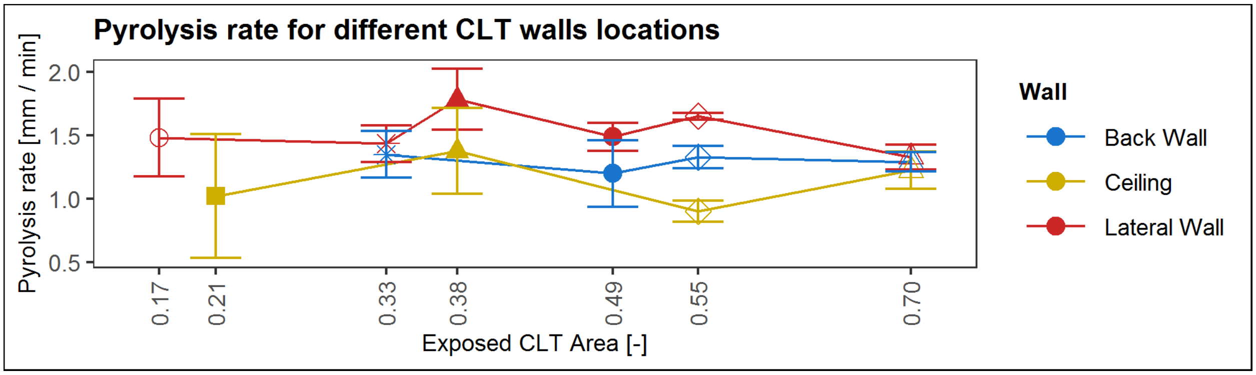

Fig. 10. Pyrolysis rates of the different timber surfaces exposed in the compartment fires.

Currently, it is a common practice to assume that the ceiling receives the biggest amount of heat and has the highest burning rate, and therefore, it is often encapsulated (i.e. protected with non-flammable materials). However, this experimental campaign presents the opposite behaviour. Due to the complexity of these experiments, it is complicated to measure oxygen concentration in different locations. However, the char layer formed in the ceiling was ~ 1.3 times thicker than the char layer of the lateral walls. This indicates that the char might have been less efficient in oxidizing and regressed less. This confirms the hypothesis of having a lower oxygen concentration in that region. Moreover, a thick char layer may diminish the heat flux arriving at the pyrolysis front, resulting in a slower pyrolysis rate and consequently in the lower burning rate of the ceiling panel.

This effect is also reflected in the heat release rate of the experiments presented in Fig. 11. The figure highlights the contribution of the burning CLT slabs to the HRR_{TOTAL} and proposes a model with a 30% reduction in the burning rate of the ceiling with respect to the other surfaces.

Fig. 11 also presents the usefulness of the fed kerosene pool fire to decouple the different sources of HRR. It is possible to observe how the "Exposed C" and "Exposed LW BW C" configurations present a smaller HRR despite having a larger exposed timber area due to the ceiling burning at a lower rate. This finding supports the normalising method using the volumetric pyrolysis rate instead of exposed CLT area, as discussed above.

The model to predict HRR_{total} is the sum of the three different sources of HRR present in the compartment: Eq. 12.

$$HRR_{total} = HRR_{fuel} + HRR_{CLT,walls} + HRR_{CLT,ceiling} \tag{12}$$

where HRR_{fuel} is the HRR of the kerosene pool fire, which is assumed to be constant across the different configuration as its burning rate was governed by the lip level [8].

Then, the HRR_{CLT} terms are substituted by their constituent variables defined in Table 1.

$$HRR_{total} = HRR_{fuel} + \rho_{CLT}\dot{p}A_{CLT,walls}\Delta H_c + \rho_{CLT}n\dot{p}A_{CLT,ceiling}\Delta H_c \pm 10\ [kw] \tag{13}$$

Variable	Description	Value
$\boldsymbol{HRR_{fuel}}$	HRR from the fuel, Kerosene pool fire.	64.5 [kW]
$\boldsymbol{\rho_{CLT}}$	Density of the CLT.	0.425 [g/mm^2]
$\dot{p}$	Average charring rate of the vertical walls.	0.025 [mm/s]
$\boldsymbol{n}$	Reduction factor ceiling pyrolysis rate.	0.7
$\boldsymbol{\Delta H_c}$	Heat of combustion of Radiata Pine.	0.013 [kJ/g]
$\boldsymbol{A_{CLT,walls}, A_{CLT,ceiling}}$	Areas of exposed timber walls and ceiling respectively.	**Input variable [m]**

Table 1

Fig. 11 shows that the proposed model captures satisfactorily the HRR trend of the experiments, including its reduction in the cases where the ceiling is present

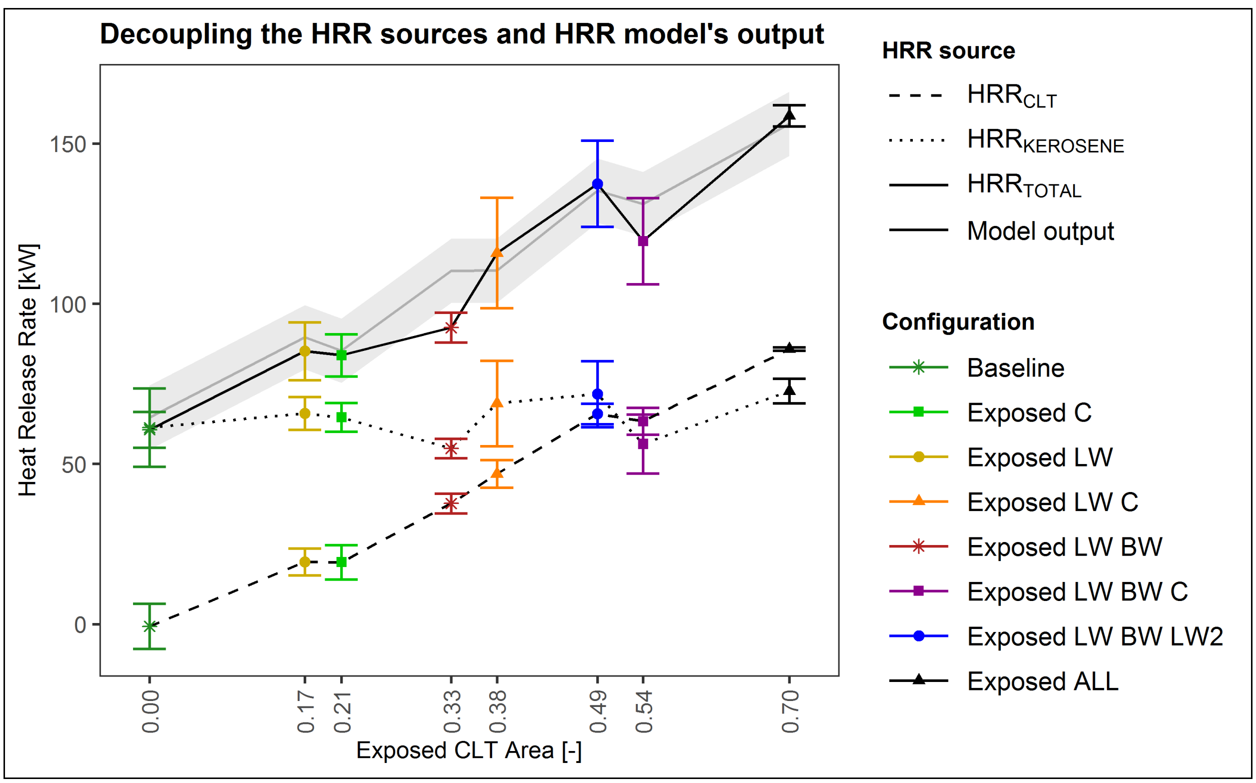

Fig. 11. Different sources of HRR that contribut to the total HRR in a CLT compartment fire for different CLT configurations. Additionally, the output of the proposed model (grey region) to predict the total HRR for this type of compartments.

In summary, these experiments outline a progressive shift towards a new fire regime (Regime-II-CLT) by introducing exposed timber surfaces to the compartment, schematically illustrated in Fig. 12. The effect of the burning timber elements consists on larger velocities at the opening (**Error! Reference source not found.**), which is a consequence of an increased momentum inside the compartment due to larger hot areas that induce buoyancy. The increased momentum and excess of pyrolysis gases prevents the oxygen from uniformly mixing across the compartment's volume, resulting in lower temperatures next to the ceiling and a descending smoke layer height. The behaviour of the gas-phase fluids has a consequence on the burning rate of the exposed timber panels, being the ceiling the surface that decomposed at the smallest rate which has also an effect on the total heat release rate of this experiments.

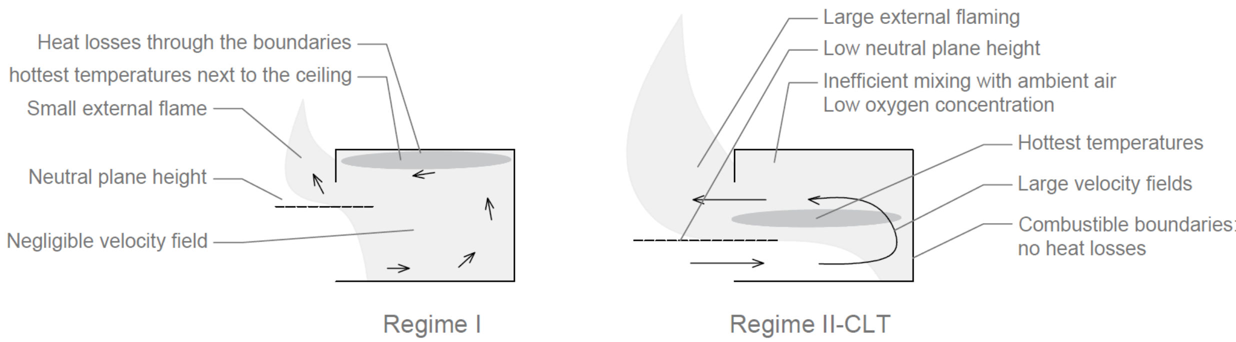

Fig. 12. Schematic representation of the physical changes that occur where CLT surfaces are exposed in a compartment fire.

5 Conclusions

This paper has investigated the effect of exposed CLT surfaces in the compartment fire dynamics development. The modification to the current calculation method to predict the temperatures inside a fully-developed compartment with timber lining has been successful. This new method captures the initial increase and later decrease in temperatures by adding exposed timber surfaces and the subsequent regime change towards a new Regime-II-CLT. Thus, exposing more CLT does not necessarily mean that the internal temperatures will be larger than in a compartment with non-combustible lining and the flow fields characteristic for a Regime-II can be achieved with the presence of burning CLT boundaries and not only by large openings. This modified calculation can now be used as a simple design approach to predict the thermal boundary to the structure and define the potential fire development.

Additionally, the change in regime triggers a lower burning rate of the ceiling compared to the other exposed timber surfaces. Therefore, exposing the ceiling results in the safest option for the design, which is contrary to the current practice. This phenomenon also implicates that timber exposure is not a function of the exposed timber area since depending on its location (ceiling vs vertical wall) the burning rate changes. Therefore, this study introduces a new way to quantify the timber exposure that includes different burning rates.

Finally, the CLT panels contribute significantly to the heat release of the fire. It is expected that the excess of pyrolysis gases from the timber panels and the induced horizontal velocities at the opening will increase and change the shape of the external flame compared to what is currently known for "conventional" compartments. This increase of external heat release rate challenges vertical compartmentation as the flame has now more energy to ignite the façade and the compartment above. Therefore, future research should study the external spilt plume emerging from compartments with exposed CLT surfaces.

6 Acknowledgements

Carmen Gorska would like to thank Juan Cuevas and Jeronimo Carrascal for their support while conducting her experiments, and to her supervisors and co-authors of this paper for their advice in the analysis of the data and writing the results. This project was funded by the Hull Family Early Career Research Fund and by the ARC Industrial Transformation Hub "Future Timber Hub" (IH150100030).

7 References

1. *Timber as a sustainable buildin material*. Timber in Ecologically Sustainable Development
2. Ferguson, I., et al., *Environmental Properties of Timber.* FWPRDC, 1996.
3. Adam Cowlard, A.B., Cecilia Abecassis-Empis, Jose Torero. *Fire safety design for tall buildings*. in *Asia-Oceania Symposium on Fire Safety and Technology*
4. Deal, S. and C. Beylert, *Correlating Preflashover Room Fire Temperatures.* Journal of Fire Protection Engineering, 1990. **2**(2): p. 33-48.
5. Thomas, P.H. and A.J. Heselden, *Fully-developed Fires in Single Compartments.* Fire Research Station, 1972. **923**.
6. Harmathy, T.Z., *A new look at compartment fires, part I.* Fire Technology, 1972. **8**(3): p. 196-217.
7. Harmathy, T.Z., *A new look at compartment fires, part II.* Fire Technology, 1972. **8**(4): p. 326-351.
8. Drysdale, D., *An introduction to fire dynamics*. Vol. 3rd. 2011, Chichester, England: John Wiley & Sons.
9. Thomas, P.H., *CIB research programmes, Building Research Establishment Paper CP32/74, BRR, Borehamwood, U.K.* 1974.
10. Torero, J.L., et al. *Revisiting the compartment fire*. in *Fire Safety Science*. 2014.
11. Thomas, P.H., Heselden, A.J. and Law, M., *Fully-developed compartment fire -two kinds of behaviour.* 1967. **18**.
12. Carmen Gorska, J.P.H., Jose L. Torero, *An Experimental Study of Medium-Scale Compartment Fire Tests with Exposed Cross Laminated Timber* 2nd International Fire Safety Symposium, Naples, Italy, June 7-9, 2017, 2017.
13. Emberly, R., et al., *Self-Extincion of Timber.* Proceeding of Combustion Institute 2016.
14. Janssens, M., *Measuring rate of heat release by oxygen consumption.* Fire Technology, 1991. **27**(3): p. 234-249.